Effect of DMSO on Protein Structure and Interactions Assessed By Collision-induced Dissociation and Unfolding

Daniel S.-H. Chan,[†] Madeline E. Kavanagh,[†] Kirsty J. McLean,[‡] Andrew. W. Munro,[‡] Dijana Matak-Vinković,[†] Anthony G. Coyne,[†] and Chris Abell*,[†]

[†]Department of Chemistry, University of Cambridge, Lensfield Road, Cambridge CB2 1EW, United Kingdom)

[‡]Centre for Synthetic Biology of Fine and Specialty Chemicals (SYNBIOCHEM), Manchester Institute of Biotechnology, School of Chemistry, The University of Manchester, Manchester M1 7DN, United Kingdom

ABSTRACT: Given the frequent use of DMSO in biochemical and biophysical assays, it is desirable to understand the influence of DMSO concentration on the dissociation or unfolding behavior of proteins. In this study, the effects of DMSO on the structure and interactions of avidin and *Mycobacterium tuberculosis* (*Mtb*) CYP142A1 were assessed through collision-induced dissociation (CID) and collision-induced unfolding (CIU) as monitored by nanoelectrospray ionization-ion mobility-mass spectrometry (nESI-IM-MS). DMSO concentrations higher than 4% (*v*/*v*) destabilize the avidin tetramer towards dissociation and unfolding, via both its effects on charge state distribution (CSD) as well as at the level of individual charge states. In contrast, DMSO both protects against heme loss and increases the stability of CYP142A1 towards unfolding even up to 40% DMSO. Tandem MS/MS experiments showed that DMSO could modify the dissociation pathway of CYP142A1, while CIU revealed the protective effect of the heme group on the structure of CYP142A1.

Over the past two decades, electrospray ionization-mass spectrometry (ESI-MS) has emerged as a powerful technique to study biomolecular structure and function.[1-2] In particular, the ability of ESI-MS to generate macromolecular ions from aqueous solution under relatively soft ionization energies has enabled the study of both non-covalent protein-protein and protein-ligand complexes under native-like conditions.[3-4] ESI-MS can moreover be interfaced with ion-mobility (IM) spectrometry, which separates gaseous ions by differences in their rotationally-averaged collision cross-section (CCS), to provide an additional dimension of resolution.[5-6]

Native mass spectrometry is an ideal technique to investigate the effects of dimethyl sulfoxide (DMSO), a co-solvent often included in biochemical and biophysical assays, on protein structure and interactions. Zenobi and co-workers reported that DMSO (0.5 to 8%) reduced the binding affinities of three protein-ligand complexes.[7] In contrast, Landreh and co-workers found that 3% DMSO stabilized the tetrameric state of transthyretin (TTR) and its non-covalent interaction with the thyroid hormone thyroxine (T4), as well as the trimeric state of the C-terminal domain of lung surfactant protein C (CTC) and its non-covalent interaction with a trivaline peptide.[8] Moreover, Williams and co-workers have investigated the effect of DMSO concentration on the structure and conformation of hen egg white lysozyme and equine myoglobin using both ESI-MS and solution phase experiments.[9] Circular dichroism (CD) spectroscopy and hydrogen-deuterium exchange (HDX) experiments suggested that the proteins underwent compaction at concentrations up to about 50%, followed by unfolding at higher concentrations.[9] In contrast, Tjernberg and co-workers have reported that DMSO concentrations as low as 3% induced destabilization, degradation and aggregation of the phosphatase domain of PFKFB1 (BPase) as revealed by both ESI-MS and solution assays.[10] Recently, our group has shown that a small compaction of protein structure by DMSO could be detected in the gas phase by the use of ESI-IM-MS.[11]

The internal energy of gaseous protein ions can be increased by raising the acceleration voltages at different stages of the mass spectrometer. Through collisions with neutral gas molecules, multiprotein complexes acquire energy and can undergo dissociation (collision-induced dissociation, CID), which commonly takes place by the ejection of a highly-charged, unfolded monomeric subunit through the asymmetric charge partitioning mechanism.[12-13] Moreover, activated protein ions can undergo unfolding (collision-induced unfolding, CIU), which can be tracked by monitoring their CCS as a function of collision energy.[14-16] Previous studies mainly by the Ruotolo group have explored the effect of various cations and ions on the CID and CIU stabilities of model proteins.[17-20] However, to our knowledge, no systematic study on the effect of DMSO on protein CID or CIU behavior has yet been reported.

In this study, avidin and CYP142A1 were chosen as representative examples of proteins with quaternary structure or prosthetic groups, respectively. Avidin is a well-

characterized glycoprotein found in the egg-white of birds and reptiles. The protein forms a multiprotein complex that consists of four identical subunits assembled together in a dimer of dimers arrangement.[21] In contrast, the *Mycobacterium tuberculosis* (*Mtb*) cytochrome P450 enzyme CYP142A1 is predominantly monomeric and binds a heme-*b* prosthetic group. CYP142A1 functions as a cholesterol oxidase and contributes to the ability of *Mtb* to establish a chronic infection.[22-24]

Our work provides evidence that DMSO influences CID and CIU stability via a dual mechanism of charge modulation as well as via charge state-independent effects. Additionally, we observe that the effects of DMSO on protein structure and interactions are highly protein-dependent, with CYP142A1 displaying unusual stability even at high DMSO concentrations. Finally, we use tandem MS/MS experiments to show that DMSO can influence the heme dissociation pathway of CYP142A1, and also demonstrate that the protective effects of the heme group on CYP142A1 stability can be tracked using CIU, a technique that should be broadly applicable to other heme-containing proteins.

□ EXPERIMENTAL SECTION

Materials and Methods. Avidin (egg white), concanavalin A (*Canavalia ensiformis*), alcohol dehydrogenase (*Saccharomyces cerevisiae*) and pyruvate kinase (rabbit heart) were obtained from Sigma-Aldrich (St. Louis, MO, USA). *Mtb* His_6-tagged CYP142A1 was expressed as previously described.[22] Protein samples were exchanged into 200 mM ammonium acetate (pH 7.0) solution using Micro Bio-Spin 6 chromatography columns (Bio-Rad, UK) and diluted to a final concentration of 20 μM (avidin) or 10 μM (CYP142A1) before analysis.

Mass Spectrometry. Nanoelectrospray ionization-ion mobility-mass spectrometry (nESI-IM-MS) was performed on a Synapt HDMS mass spectrometer (Waters, Manchester, UK) modified for studying high masses and equipped with a traveling-wave (TW) IMS device. 2.5 μL of protein solution was injected into a gold-coated borosilicate emitter (Thermo Scientific, UK) for sampling. Typical conditions were: capillary voltage 1.5 kV, cone voltage 50 V, transfer collision voltage 12 V, source temperature 20 °C, backing pressure 3–4 mbar, trap pressure 3–4 × 10^{-2} mbar, IMS (N_2) pressure 5–6 × 10^{-1} mbar and TOF pressure 7–8 × 10^{-7} mbar. To effect CID and CIU, the trap collision voltage was raised in 5 V increments from 20 to 100 V for avidin and in 10 V increments from 20 to 150 V for CYP142A1. To record CIU, the instrument was operated in mobility TOF mode using an IMS wave velocity of 250 ms^{-1} and a wave height of 10 V. Avidin, concanavalin A, alcohol dehydrogenase and pyruvate kinase were used as calibrant ions for CCS determination.

Data Processing. Mass spectra were calibrated externally using a solution of cesium iodide (100 mg mL^{-1}). Data acquisition and processing were performed using MassLynx 4.1 (Waters) and DriftScope 2.5 (Waters). For CID analysis, the measured peak heights were used and all charge states were taken into account. CID50 values were calculated from non-linear curve fitting using Origin 9.1 (OriginLab). PULSAR[16] was used to calibrate CCS values,[25] visualize CIU fingerprints and calculate CIU50 values. Unless otherwise stated, all CCS values are quoted as N_2 values. CID50 and CIU50 values are quoted as mean ± standard deviation of at least two independent experiments.

As algorithms for CCS calculation from X-ray crystal structures are parameterized for helium collision gas,[26] the corresponding CCS(He) of CYP142A1 was also determined by calibration with helium CCS values in order to enable comparison between the experimental result and the theoretical CCS. The experimental CCS(He) of CYP142A1 was 3140 $Å^2$, which is within 2% of the theoretical $CCS(He)_{calc}$ value of 3090 $Å^2$, where $CCS(He)_{calc} = 1.14 \times CCS(He)_{PA} \times (M_{exp}/M_{PDB})^{2/3}$ and $CCS(He)_{PA}$ is the CCS calculated from the X-ray crystal structure of CYP142A1 (PDB: 2XKR)[22] using the projection approximation (PA) algorithm implemented in DriftScope, M_{exp} is the mass of His_6-tagged CYP142A1 (47178 Da) used in the experiment and M_{PDB} is the mass of the CYP142A1 construct (45015 Da) in the reported crystal structure. The coefficient of 1.14 in the above calculation is an empirically determined scaling factor that takes into account the underestimation of CCS by the PA algorithm due to its masking of the cavity slow-down effect.[2, 26]

□ RESULTS AND DISCUSSION

DMSO Affects The Charge of Protein Ions in the Gas Phase. The bimodal effect of DMSO on protein charging has been well-documented in the literature. At low concentrations, DMSO reduces protein charge, which has been attributed to a global compaction of protein structure in solution by the groups of Voets[27] and Williams[9] on the basis of CD spectroscopy, small-angle neutron scattering, Rayleigh scattering and HDX-MS results. Our group has recently shown that the compaction of protein structure by DMSO can also be detected in the gas phase through the use of nESI-IM-MS, even at the level of individual charge states.[11] At high DMSO concentrations, DMSO increases protein charge, which has been attributed to protein denaturation.[28] However, to our knowledge, the use of nESI-IM-MS to study the effect of high DMSO concentrations on protein structure has not previously been reported.

In this study, the effect of DMSO concentration on avidin and CYP142A1 under minimal activation conditions was first investigated. Concentrations of DMSO higher than 60% could not be examined due to aggregation of avidin, whereas for CYP142A1 the maximum DMSO concentration that could be tested was 40%. The tetrameric state of avidin was well-preserved at concentrations up to 60% DMSO (Figure S1a). At 50 and 60% (*v*/*v*) DMSO, a small amount of monomeric avidin ions (16 kDa) could be

detected centered around the 9+ charge state. This result suggests that high concentrations of DMSO could induce the dissociation of avidin even under minimal activation conditions.

For CYP142A1, the native mass spectra showed that CYP142A1 exists predominantly in monomeric form (Figure S2a), consistent with the reported X-ray crystal structure,[22] and was centered around the 12+ charge state in the absence of DMSO. The protein remained monomeric as the DMSO concentration was increased to 40%. However, signals of individual charge states were broadened, which could be attributed to the adduction of small molecules to the protein at higher DMSO concentrations. Moreover, CYP142A1 fully retained its heme moiety even at 40% DMSO, in contrast to a previous ESI-MS study of myoglobin in which 90% of heme was already lost at 20% DMSO.[9] To our knowledge, this is the first reported study of CYP142A1 by native MS.

The bimodal effect of DMSO on protein charge was also evident (Figures S1b and S2b). However, very high DMSO concentrations (50% for avidin and 40% for CYP142A1) decreased average charge slightly, similar to previously observed for lysozyme and myglobin.[9] Intriguingly, the average charge of CYP142A1 reached at 30% or 40% DMSO was still lower than under DMSO-free conditions (Figure S2b), in contrast to avidin where supercharging was observed from 10% of DMSO (Figure S1b). To our knowledge, CYP142A1 is the first protein that has been reported to remain charge-reduced at such high DMSO concentrations. In a previous study, avidin, concanavalin A, alcohol dehydrogenase and pyruvate kinase were supercharged at DMSO concentrations greater than 10 or 20%.[11] Meanwhile, the onset of supercharging was around 20% DMSO for lysozyme and myoglobin,[9] while for BPase both supercharging and protein denaturation were evident at as little as 3% of DMSO.[10] As DMSO is less volatile than water, electrospray droplets actually become enriched (estimated to be 3 to 5-fold[9]) in DMSO as they shrink. In concert with the IM-MS data (see below), our data suggest that CYP142A1 may remain compacted at DMSO concentrations even higher than 40% when in the gas phase. The reason for the remarkable gas-phase stability of CYP142A1 under such high DMSO concentrations is not known.

DMSO Influences The Size of Individual Protein Charge States. IM-MS was also performed to assess the effect of DMSO concentration on the size of avidin and CYP142A1 ions. The weighted-average CCS of CYP142A1 at 0% DMSO was within 2% (see Experimental Section) of the theoretical CCS predicted from the X-ray crystal structure (PDB: 2XKR),[22] suggesting that CYP142A1 retained its native structure in the gas phase. The abundance-weighted average CCS of avidin tetramers decreased from 4080 Å^2 without DMSO to 4010 Å^2 at 4% DMSO (Figure S1b), while for CYP142A1 the CCS decreased from 3450 Å^2 without DMSO to 3240 Å^2 at 20% DMSO (Figure S2b). This is consistent with the compaction of protein structure at low DMSO concentrations as shown previously by IM-MS[11] or solution-phase techniques.[9, 27]

Increasing the DMSO concentration beyond 4% led to an increase in average CCS for avidin, initially mirroring the trend for average charge (Figure S1b). However, the two trends deviated at higher DMSO concentrations, with CCS continuing to rise as the DMSO concentration was increased beyond 40%, even while average charge decreased. The maximal CCS of avidin tetramers (4240 Å^2) was reached at 60% DMSO. This CCS was 4% larger than the average size of ions in the absence of DMSO (4080 Å^2), and 6% larger than the compacted avidin ions at 4% DMSO (4010 Å^2). For CYP142A1, the change in average CCS of CYP142A1 ions generally paralleled the trend for charge, except that the minimum CCS (3240 Å^2) was reached at 20% DMSO, instead of at 4% DMSO for minimum charge (Figure S2b). Moreover, the average CCS at 40% DMSO (3350 Å^2) was still 3% lower than that in the absence of DMSO, suggesting that the overall structure of CYP142A1 was still compacted even at the highest DMSO concentration used.

To investigate whether the change in CCS at higher DMSO concentrations could be related to conformational changes of individual ions, the CCS of individual charge states were plotted against DMSO concentration. Higher DMSO concentrations generally increased the CCS of individual avidin charge states, with the exception of 4% DMSO where a minimum in CCS was observed (Figures S3a). Individual charge states of CYP142A1 were also compacted by DMSO, with minimum CCS values being reached at 20% DMSO for all charge states (Figure S3b). These data therefore suggest that DMSO could induce expansion or compaction of avidin and CYP142A1 ions, respectively, even at the level of individual charge states. We hence propose that the increase in average CCS of avidin induced by DMSO (Figure S1b) could arise from a combination of two factors. Firstly, the supercharging effect of DMSO allows avidin ions to access higher charge states that are also larger due to increased Coulombic repulsion. Secondly, DMSO causes expansion in the size of individual charge states, which is presumably related to its denaturing ability. Conversely, DMSO is proposed to reduce the average CCS of CYP142A1 (Figure S2b) both as consequence of its ability to shift the charge state distribution (CSD) of CYP142A1 to lower charge, as well as its ability to compact protein structure at the level of individual charge states.

DMSO Modulates the CID Stability of Proteins and Influences the Heme Dissociation Pathway of CYP142A1. Several research groups have studied the effect of DMSO on the stability of non-covalent interactions by ESI-MS. In one study, DMSO (0.5 to 8%) weakened the stability of three different protein-ligand complexes, which was attributed to the ability of DMSO to destabilize the protein and perturb the ligand-binding pocket, interfere with the ligand, or act as a competing inhibitor.[7] In contrast, another study reported a protective effect of DMSO (3%) on both the quaternary structure of multiprotein complexes and their interaction with small molecule or peptide ligands, which was attributed to a combination of charge reduction and a cooling effect from adduct dissociation.[8] However, no systematic study has been performed on the effect of high concentrations of DMSO on the CID stability of protein structure and interactions in the literature.

In this study, avidin tetramers underwent CID at higher trap collision voltages (CV) to generate highly charged, unfolded monomers and "stripped" trimers (Figure 1a). In the absence of DMSO, ~50% of the tetramer was dissociated at a trap CV of 65 V. Moreover, higher charge states of avidin became depleted first as the collision voltage was raised, which could be attributed to increased Coulombic repulsion. When DMSO was added, the overall CID pathway did not change and similar distributions of monomers and trimers were produced (Figure 1b shows CID spectra at 60% DMSO). However, dissociation was facilitated by higher DMSO concentrations. For instance, in the absence of DMSO, 77% of the tetramer was preserved at a CV of 60 V, whereas with 60% DMSO, only 17% of the tetramer remained intact at the same CV. Plotting the abundance of the tetramer as a function of CV (Figure 1c) reveals that DMSO concentrations higher than 4% promoted tetramer dissociation. The Figure 1c inset presents CID50 values (the CV needed to dissociate 50% of tetramers) as a function of DMSO concentration. The CID50 of avidin tetramers increased from 66.5 to 78.1 V (+11.6 V) as the DMSO concentration was raised from 0 to 4%, indicating a protective effect against dissociation. However, further increase in the DMSO concentration led to a decrease in CID50, with the minimum CID50 value of 53.6 V being reached at 50% DMSO, corresponding to a decrease of 12.9 V compared to in the absence of DMSO. In summary, our data show that high concentrations of DMSO have a significant destabilizing effect on the CID of avidin. Only at 4% DMSO, where the average charge of the avidin tetramer was lowest, did DMSO have a protective effect against subunit dissociation.

Generally, the CID50 values of avidin were inversely related to average protein charge. That is, DMSO concentrations that produced higher average charges of the avidin tetramer also gave lower overall CID50 values. Therefore, it was also of interest to determine whether the destabilization of avidin tetramers by DMSO was due solely to the ability of DMSO to shift the CSD of avidin tetramers towards higher charge, or whether DMSO also exerted

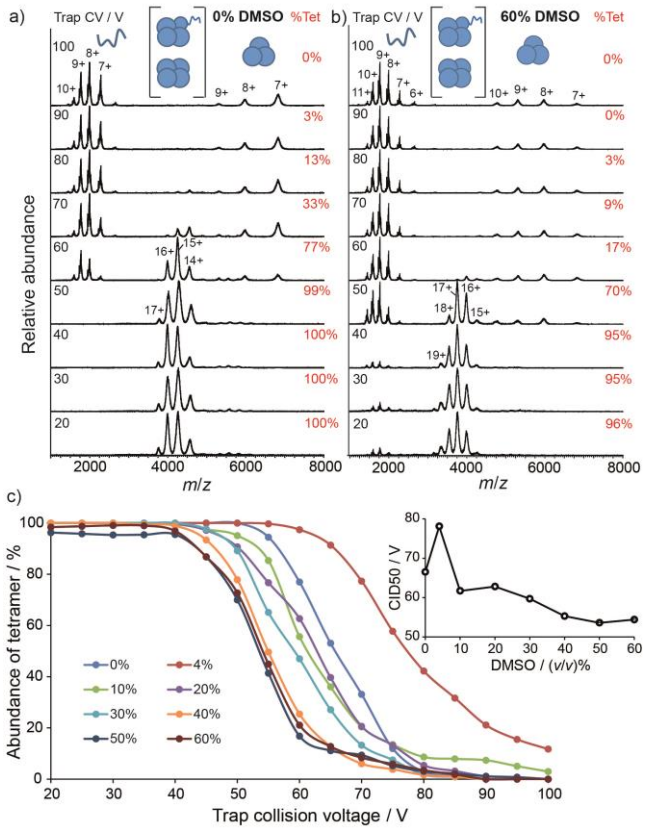

Figure 1. DMSO influences the CID stability of avidin. Native MS spectra of avidin in the presence of a) 0% or b) 60% DMSO at different trap CVs. The abundance of the tetramer (%Tet) at each CV is indicated. c) Abundance of tetramer as a function of trap CV at each DMSO concentration. The inset shows the CID50 as a function of DMSO concentration.

destabilizing effects on individual ions that are independent of its effect on CSD. To address this, the CID50 values for the individual charge states were plotted as a function of DMSO concentration (Figure S4a). Interestingly, DMSO also promoted the dissociation of individual charge states. For example, the CID50 of the 16+ charge state was lowered from 1043 to 954 eV (–89 eV) when the DMSO concentration was raised from 0 to 60%, while for the 17+ charge state a reduction from 1020 to 923 eV (–97 eV) in CID50 was observed upon increasing DMSO concentration from 20 to 60%. This is in contrast to previously reported results from Landreh and co-workers, where 3% DMSO had no effect on the CID stability of the 16+ charge state of TTR.[8] However, our study used relatively high concentrations of DMSO, compared to the 3% DMSO used for TTR. Indeed, the protective effect of 4% DMSO against dissociation could not be detected at the level of individual charge states in our study (Figure S4a). Taken together, the overall reduction in the CID stability of avidin at high DMSO concentrations could be attributed to two, possibly interrelated, mechanisms. First, DMSO shifts the CSD of avidin tetramers towards ions of higher charge, which have lower intrinsic stability against dissociation. Second, DMSO may also exert a destabilizing effect against individual charge states, presumably as a consequence of its denaturing effect.

The influence of DMSO on the CID behavior of CYP142A1 was also investigated. Figures 2a and 2b show CID spectra of CYP142A1 at 0 and 30% DMSO, respectively. CYP142A1 holoenzyme underwent CID to release the apoenzyme and also the free heme-*b* ion at *m*/*z* 616 Da ($[M]^+$) together with an ammonia adduct of heme-*b* at *m*/*z* 633 Da ($[M+NH_3]^+$). The CYP142A1 peaks also generally became sharper at higher CV, consistent with the dissociation of buffer and/or DMSO molecules from the protein. Interestingly, DMSO had a protective effect against heme loss. For instance, only 20% of CYP142A1 ions retained heme at 140 V in the absence of DMSO (Figure 2a), whereas in the presence of 30% DMSO, the proportion of the holoenzyme was 37% (Figure 2b). Among all DMSO concentrations tested, heme dissociation occurred earliest at 0% DMSO (Figure 2c), with a CID50 value (the CV needed to dissociate 50% of holoenzyme) of 117.7 V (Figure 2c inset). The highest stability of the holoenzyme was observed at 4% DMSO (CID50 = 137.9 V), with stability decreasing as the DMSO concentration was increased further.

As with avidin, it was also of interest to explore whether DMSO could protect against dissociation of the heme group in a manner that is independent of its effects on CSD. To study this issue further, tandem MS/MS was performed to study the dissociation pathways of individual charge states. In the absence of DMSO, CYP142A1 ions exhibited two heme dissociation pathways: charge stripping and charge retention (Figure 3a). In the charge stripping pathway, the holo-CYP142A1 *N*+ ion dissociates into the heme monocation and the (*N* – 1)+ ion of the apoenzyme. This is the anticipated dissociation pathway for CYP142A1 because the protein is expressed in the ferric (3+) oxidation state, and therefore would be expected to dissociate the $(Fe(III)heme)^+$ ion.[29] In contrast, in the charge retention pathway, the liberated apoenzyme has the same charge as the initial holoenzyme, which is presumed to occur via the dissociation of a neutral heme species, possibly a heme-acetate adduct.[30] However, at 30% DMSO, the charge retention pathway is eliminated and only the charge stripping pathway is observed (Figure 3b). We reason that the much higher concentration of DMSO (*ca.* 4.2 M) relative to acetate (200 mM) causes the anionic acetate to be displaced from heme in the initial solution through the formation of a $(heme\text{-}DMSO)^+$ adduct,[31-32] thereby eliminating the charge retention pathway. In contrast, avidin tetramers exhibited only a minor amount of charge stripping before dissociation (Figure S5).

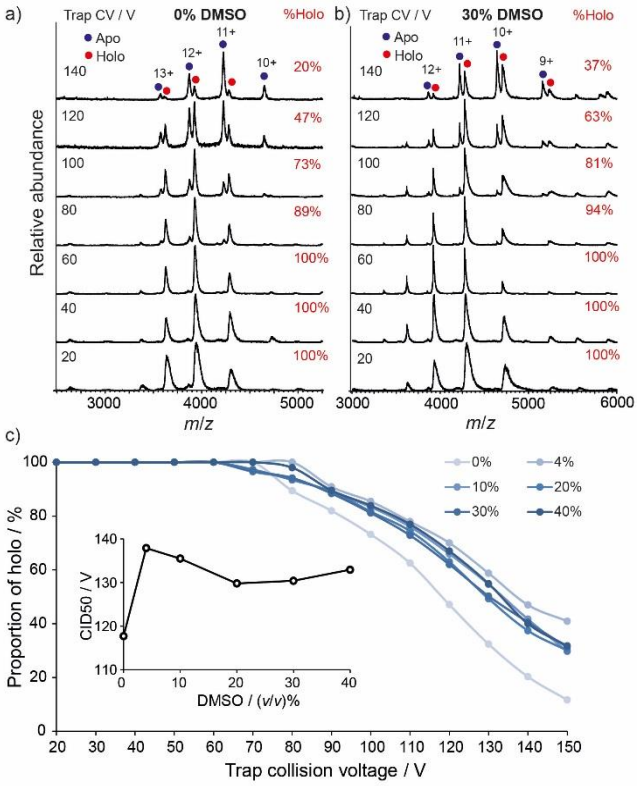

Figure 2. DMSO influences the CID stability of CYP142A1. Native MS spectra of CYP142A1 in the presence of a) 0% or b) 30% DMSO at different trap CVs. The proportion of holo-CYP142A1 (%Holo) at each CV is indicated. c) Proportion of holo-CYP142A1 as a function of trap CV at each DMSO concentration. The inset shows the CID50 as a function of DMSO concentration.

The MS/MS data also confirmed that higher charge states of CYP142A1 dissociated heme more easily than lower charge states, as expected (Figures 3c and S6a). Moreover, DMSO conferred a protective effect against heme-*b* loss even at the level of individual charge states. For instance, the CID50 values of the 11+ and 12+ charge states increased from 1297 ± 13 eV to 1421 ± 18 V (+124 eV) and from 1277 ± 17 eV to 1354 ± 16 eV (+77 eV) respectively as the DMSO concentration was raised from 0 to 30% (Figure 3c inset). Taken together, these data suggest that DMSO protects against heme loss both by shifting the CSD of CYP142A1 towards ions of lower charge, which have higher intrinsic stability to dissociation, as well as by enhancing the stability of individual charge states. The latter effect could be linked to the compaction of CYP142A1 ions by DMSO concentrations, that is, more compact holoenzymes have a greater resistance against heme loss.

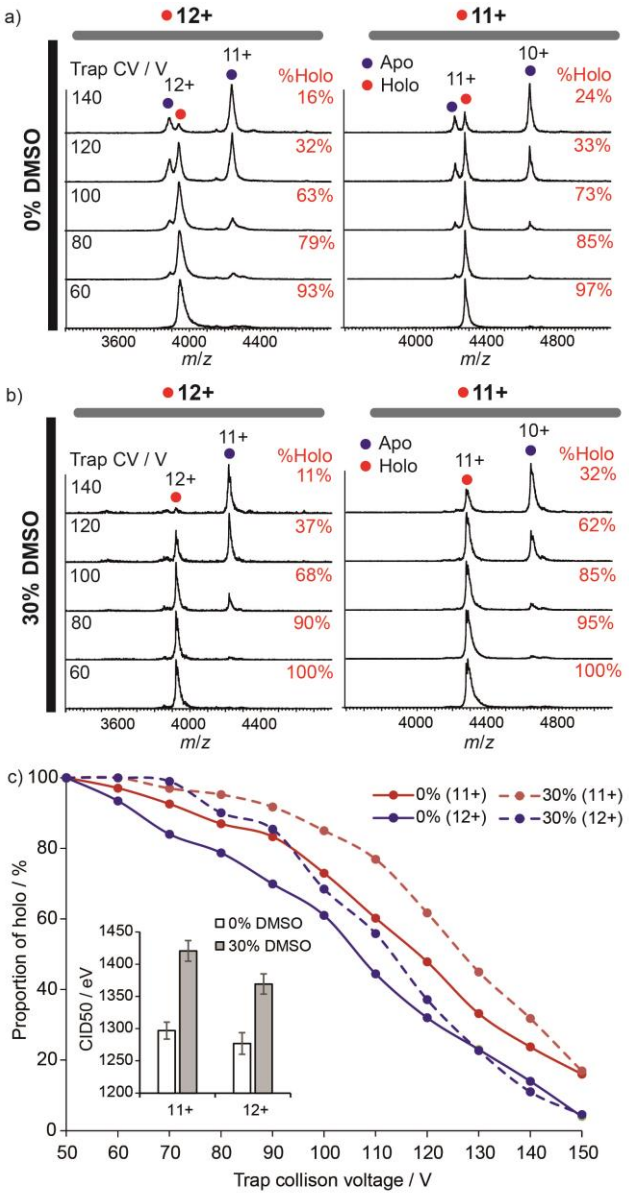

Figure 3. DMSO influences the dissociation pathway of CYP142A1. Tandem MS/MS of CYP142A1 at a) 0% DMSO and b) 30% DMSO with selection of the 12+ holoenzyme (left panel) or 11+ holoenzyme (right panel) as the precursor ion (indicated by a filled red circle). The trap CV and proportion of holo-CYP142A1 (%Holo) at each CV is indicated. c) Proportion of holo-CYP142A1 as a function of trap CV at 0 or 30% DMSO for 11+ and 12+ charge states. The inset shows the CID50 for the 11+ and 12+ charge states at 0 and 30% DMSO.

DMSO Modulates the CIU Stability of Proteins. A number of studies have investigated the effect of various solution additives on the CIU stability of different proteins. The Ruotolo group have shown that both anions[17] and cations[18] can have dramatic effects on both CIU and

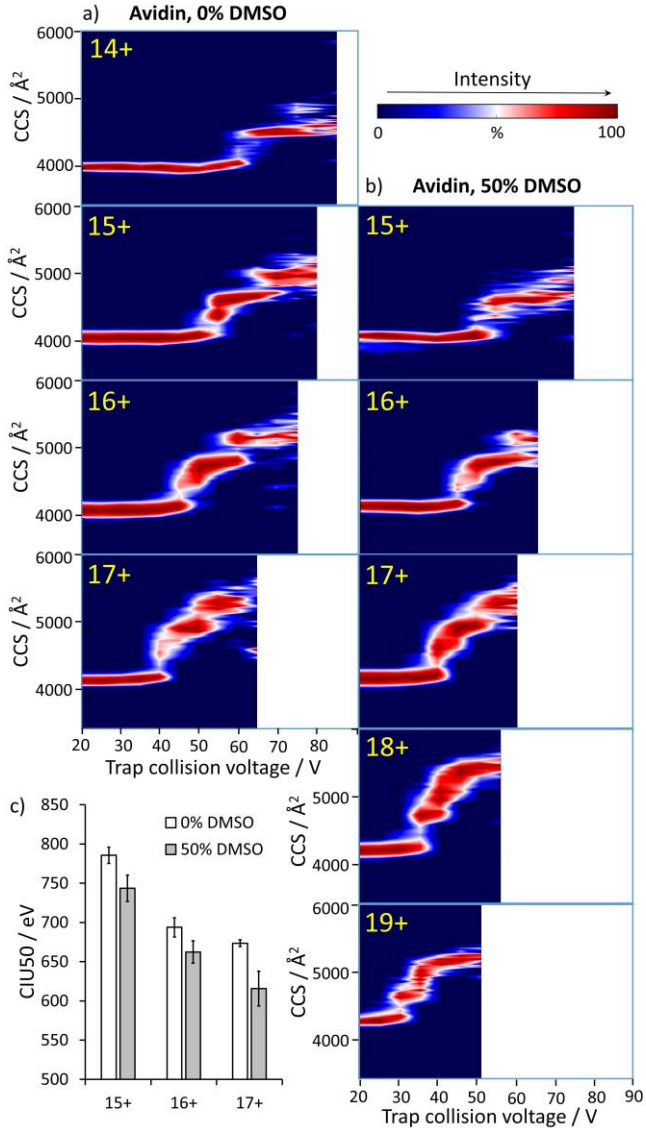

Figure 4. DMSO affects the CIU stability of avidin. CIU fingerprints of avidin tetramer charge states in the presence of a) 0% or b) 50% DMSO. c) CIU50 values for the 15+, 16+ and 17+ charge states at 0 and 50% DMSO.

CID stabilities. It was postulated that anions stabilize proteins through dissociative cooling-type mechanisms, whereas cations increase stability by forming multidentate interactions within proteins to tether together non-contiguous protein regions.[19] Robinson, Ruotolo and co-workers have found that TrisH$^+$ also increased CIU stability, which was attributed to an evaporative cooling mechanism or alternatively to the binding of TrisH$^+$ to critical regions of the protein so as to replace solvent contacts that are needed for maintaining native-like conformations.[20] However, to our knowledge, the effect of DMSO on the CIU stability of proteins has not yet been reported in the literature.

Figure 4a shows CIU fingerprints for the 14+ to 17+ charge states of the avidin tetramer in the absence of DMSO. At least three less compact conformations in addition to the native conformation were observed at 0% DMSO for the 15+ charge state of avidin, which was similar to previously reported.[19-20] Higher charge states of the avidin tetramer unfolded at lower CV, which can again be attributed to increased Coulombic destabilization. Unfolding pathways for the avidin tetramer were broadly similar in the presence of 50% DMSO (Figure 4b). However, lower voltages were needed to unfold avidin ions of a given charge state at 50% DMSO compared to in the absence of DMSO. For instance, the CIU50 (energy needed to deplete 50% of the most compact conformation) value of the 15+ ion of the avidin tetramer decreased from 786 ± 11 eV in the absence of DMSO to 744 ± 17 V (−42 eV) with 50% DMSO (Figures 4c and S4b). However, the decreases in CIU50 induced by DMSO are comparatively smaller than the reductions of CID50 described previously (Table S1), indicating that DMSO has a greater destabilizing effect on tetramer dissociation than unfolding.

The collision energy differences between CID50 and CIU50 were invariably positive (Figure S4c), indicating that all charge states of the avidin tetramer undergo unfolding before dissociation, consistent with the asymmetric protein dissociation hypothesis. The magnitudes of these differences were comparable to a previous CID/CIU study on avidin by Ruotolo and co-workers.[33] Moreover, at DMSO concentrations between 0 and 30%, the collision energy difference generally increased with charge state, similar to previous observations.[33] As both CID and CIU values decrease with charge, this suggests that Coulombic repulsion has a larger destabilizing effect on unfolding compared to dissociation. However, the collision energy differences were generally reduced at high DMSO concentrations (≥40%). For example, the collision energy difference for the 16+ charge state of avidin was decreased from 404 ± 40 eV at 20% DMSO to 313 ± at 31 eV at 60% DMSO. This observation is consistent with the greater ability of DMSO at promote dissociation compared to unfolding of individual charge states, as noted above.

CIU fingerprints for the 10+ to 13+ charge states of the CYP142A1 holoenzyme at 0 and 30% DMSO are shown in Figures 5a and 5b, respectively. As with avidin, CYP142A1 holoenzymes transitioned through progressively more extended conformers as the CV was increased, with the exception of the 10+ ion which exhibited only two conformational states (compact and extended) over the range of CV tested. Unlike with avidin, however, DMSO increased the stability of CYP142A1 ions against unfolding. For instance, the CIU50 value of the 11+ holoenzyme increased from 650 ± 15 eV at 0% DMSO to 696 ± 9 V (+46 eV) at 30% DMSO (Figures 5c and S6b). Thus, and in similar fashion to its effect on CID stability, it is proposed that DMSO increases the stability of CYP142A1 holoenzymes against unfolding both by reducing the average charge of the ions, as well as by increasing the CIU stability at the level of individual charge states. However, the

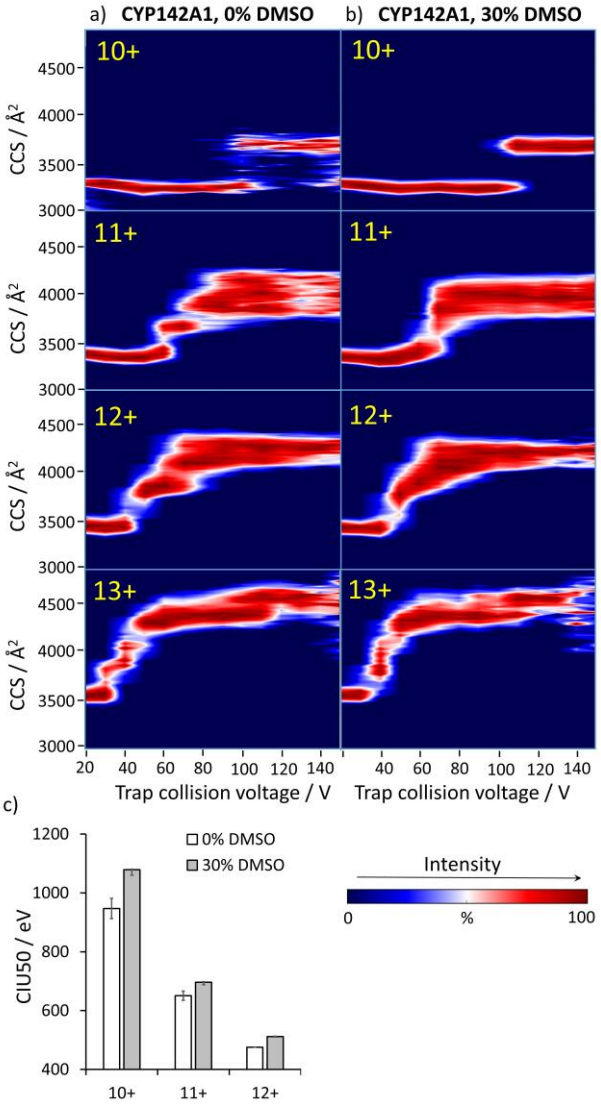

Figure 5. DMSO affects the CIU stability of CYP142A1. CIU fingerprints of CYP142A1 holoenzyme charge states in the presence of a) 0% or b) 30% DMSO. c) CIU50 values for the 10+, 11+ and 12+ charge states at 0 and 30% DMSO.

increases in CIU50 induced by DMSO are relatively small compared to the increases of CID50 described above (Table S1). Figure S6c plots the collision energy differences between CID50 and CIU50 for different charge states of the CYP142A1 holoenzyme. As with avidin, CYP142A1 holoenzymes generally unfold before dissociating, and the collision energy differences at lower charge states were also reduced. This is consistent with the observation that DMSO has a greater protective effect on CID compared to CIU, as noted above.

The unfolding behavior of the ejected CYP142A1 apoenzyme was also tracked. CIU fingerprints of the apoenzymes were similar in the absence (Figure S7a) or presence of 30% DMSO (Figure S7b). At 30% DMSO, the 9+ apoenzyme was ejected in a compact state (CCS = 3060 Å²) that did not unfold even at the highest CV tested. The ejected 10+ apoenzyme was also initially compact (CCS =

3180 Å^2), but transitioned to an extended conformation (CCS = 3620 Å^2) at voltages beyond 90 V. These CCS values are similar to those for the compact and extended states of the 10+ holoenzyme at the same CV (CCS = 3200 and 3640 Å^2 respectively), indicating that the loss of the heme group did not have a major effect on the size of either the compact or extended conformations of CYP142A1. The 11+ to 13+ charge states of the apoenzyme were ejected in extended states.

Monitoring the Protective Effect of the Heme Group using CIU. The heme prosthetic group is known to stabilize the structure of heme-containing proteins, including cytochrome P450s.[34] Using ultraviolet photodissociation (UVPD) mass spectrometry, Brodbelt and Cammarata showed that the cleavage of holo-myoglobin was suppressed in regions that interact with heme, indicating that the heme had a protective effect against fragmentation.[35] Williams and co-workers found that the heme group protected against the DMSO-induced unfolding of myoglobin by solution-phase HDX-MS experiments.[9] Intriguingly, the stabilizing effect of the heme group on the unfolding stability of CYP142A1 could also be monitored by CIU. For instance, at 0% DMSO, the CIU50 value for the 10+ holoenzyme was 947 ± 3 eV, but this decreased to 852 ± 2 eV (−95 eV) for the 10+ apoenzyme (Figure S7c). Similarly, at 30% DMSO the CIU50 value for the 10+ holoenzyme (1079 ± 20 eV) was 204 eV higher than for the 10+ apoenzyme (875 ± 14 eV). These results indicate that the heme group substantially stabilizes the CYP142A1 holoenzyme in the gas phase. However, while high DMSO concentrations protected against the unfolding of the holoenzyme, it had little effect on the unfolding stability of the corresponding apoenzyme (Figure S7d).

□ CONCLUSIONS

Native nESI-IM-MS has been used to study the effect of DMSO on the dissociative and unfolding stability of avidin and *Mtb* CYP142A1. To our knowledge, this is the first systematic study of the effect of DMSO on protein CID and CIU in the literature. There are a number of general conclusions from our work.

We have provided evidence that suggests a dual mechanism for the ability of DMSO to modulate the CID and CIU stability of proteins. DMSO not only shifts the CSD of proteins to higher or lower charge states, which vary in intrinsic stability due to differences in electrostatic repulsion, but also modulates stability via effects at the level of individual charge states.

Our data also show that the effects of DMSO on protein structure and interactions are highly protein-dependent, which has implications for the design of biological assays where DMSO is frequently employed as a co-solvent. While DMSO concentrations higher than 4% facilitated the dissociation and unfolding of the avidin tetramer, CYP142A1 exhibited remarkable stability in the presence of up to 40% DMSO, which protected the enzyme from both heme loss and unfolding. To our knowledge, CYP142A1 is the first protein that has been reported to remain charge-reduced at such high DMSO concentrations in native MS. However, compared to previous work with ions,[17-19] the stabilizing effects of DMSO on CYP142A1 are comparatively weaker. This could be due to the fact that as DMSO is neutral, it interacts relatively weakly with protein, and hence less energy is removed when DMSO adducts dissociate from the protein.

Additionally, we have established using tandem MS/MS experiments that DMSO could modify the heme dissociation pathway of CYP142A1. In the absence of DMSO, CYP142A1 can dissociate either the positive $(Fe(III)\text{-heme})^+$ ion or the neutral (Fe(III)heme)–acetate adduct, resulting in charge stripping and charge retention, respectively. However, DMSO is hypothesized to displace acetate, such that only the charge stripping pathway is observed in the presence of DMSO. Finally, we have demonstrated that the protective effects of the heme group on the gas-phase stability of CYP142A1 can be assessed using CIU. We envisage that this approach could be broadly applied to study the stabilizing effect of heme or other prosthetic groups on other proteins in the gas phase.

ASSOCIATED CONTENT

Supporting Information

Native MS of avidin at different DMSO concentrations showing average charge and CCS (Figure S1); native MS of CYP142A1 at different DMSO concentrations showing average charge and CCS (Figure S2), CCS of avidin tetramers and CYP142A1 as a function of DMSO concentration (Figure S3); CID50 and CIU50 values of avidin tetramers as a function of DMSO concentration (Figure S4); tandem MS/MS of avidin tetramers (Figure S5); CID50 and CIU50 values of CYP142A1 as a function of DMSO concentration (Figure S6); CIU fingerprints of CYP142A1 apoenzyme (Figure S7); CID50 and CIU50 values of selected avidin and CYP142A1 charge states (Table S1) (PDF).

AUTHOR INFORMATION

Corresponding Author

*E-mail: ca26@cam.ac.uk.

ACKNOWLEDGMENT

The authors thank Timothy D. Allison (University of Oxford) for assistance with PULSAR. D.S.-H.C. acknowledges the Croucher Foundation and the Cambridge Commonwealth, European and International Trust for receipt of a Croucher Cambridge International Scholarship. M.E.K. was supported by a Commonwealth (University of Cambridge) Scholarship awarded in conjunction with the Cambridge Commonwealth Trust and Cambridge Overseas Trust. K.J.M. and A.G.C. were supported by grants from the UK BBSRC (Biotechnology and Biological Sciences Research Council (BB/I019669/1 and BB/I019227/1).

REFERENCES

1. Rajabi, K.; Ashcroft, A. E.; Radford, S. E., *Methods* **2015,** *89*, 13-21.

2. Benesch, J. L. P.; Ruotolo, B. T., *Curr. Opin. Struct. Biol.* **2011,** *21*, 641-649.
3. Hilton, G. R.; Benesch, J. L. P., *J. R. Soc. Interface* **2012,** *9*, 801-816.
4. Mehmood, S.; Allison, T. M.; Robinson, C. V., *Annu. Rev. Phys. Chem.* **2015,** *66*, 453-474.
5. Lanucara, F.; Holman, S. W.; Gray, C. J.; Eyers, C. E., *Nat. Chem.* **2014,** *6*, 281-294.
6. Konijnenberg, A.; Butterer, A.; Sobott, F., *Biochim. Biophys. Acta* **2013,** *1834*, 1239-1256.
7. Cubrilovic, D.; Zenobi, R., *Anal. Chem.* **2013,** *85*, 2724-2730.
8. Landreh, M.; Alvelius, G.; Johansson, J.; Jörnvall, H., *Anal. Chem.* **2014,** *86*, 4135-4139.
9. Sterling, H. J.; Prell, J. S.; Cassou, C. A.; Williams, E. R., *J. Am. Soc. Mass Spectrom.* **2011,** *22*, 1178-1186.
10. Tjernberg, A.; Markova, N.; Griffiths, W. J.; Hallén, D., *J. Biomol. Screen.* **2006,** *11*, 131-137.
11. Chan, D. S.-H.; Matak-Vinković, D.; Coyne, A. G.; Abell, C., *ChemistrySelect* **2016,** *1*, 5686-5690.
12. Jurchen, J. C.; Williams, E. R., *J. Am. Chem. Soc.* **2003,** *125*, 2817-2826.
13. Jurchen, J. C.; Garcia, D. E.; Williams, E. R., *J. Am. Soc. Mass Spectrom.* **2004,** *15*, 1408-1415.
14. Hopper, J. T. S.; Oldham, N. J., *J. Am. Soc. Mass Spectrom.* **2009,** *20*, 1851-1858.
15. Eschweiler, J. D.; Rabuck-Gibbons, J. N.; Tian, Y.; Ruotolo, B. T., *Anal. Chem.* **2015,** *87*, 11516-11522.
16. Allison, T. M.; Reading, E.; Liko, I.; Baldwin, A. J.; Laganowsky, A.; Robinson, C. V., *Nat. Commun.* **2015,** *6*, 8551.
17. Han, L.; Hyung, S.-J.; Mayers, J. J. S.; Ruotolo, B. T., *J. Am. Chem. Soc.* **2011,** *133*, 11358-11367.
18. Han, L.; Hyung, S.-J.; Ruotolo, B. T., *Angew. Chem. Int. Ed.* **2012,** *51*, 5692-5695.
19. Han, L.; Ruotolo, B. T., *Int. J. Ion Mobil. Spec.* **2013,** *16*, 41-50.
20. Freeke, J.; Bush, M. F.; Robinson, C. V.; Ruotolo, B. T., *Chem. Phys. Lett.* **2012,** *524*, 1-9.
21. Livnah, O.; Bayer, E. A.; Wilchek, M.; Sussman, J. L., *Proc. Natl. Acad. Sci. USA* **1993,** *90*, 5076-5080.
22. Driscoll, M. D.; McLean, K. J.; Levy, C.; Mast, N.; Pikuleva, I. A.; Lafite, P.; Rigby, S. E. J.; Leys, D.; Munro, A. W., *J. Biol. Chem.* **2010,** *285*, 38270-38282.
23. Ouellet, H.; Johnston, J. B.; Ortiz de Montellano, P. R., *Trends Microbiol.* **2011,** *19*, 530-539.
24. Pandey, A. K.; Sassetti, C. M., *Proc. Natl. Acad. Sci. U.S.A.* **2008,** *105*, 4376-4380.
25. Ruotolo, B. T.; Benesch, J. L. P.; Sandercock, A. M.; Hyung, S.-J.; Robinson, C. V., *Nat. Protocols* **2008,** *3*, 1139-1152.
26. D'Atri, V.; Porrini, M.; Rosu, F.; Gabelica, V., *J. Mass Spectrom.* **2015,** *50*, 711-726.
27. Voets, I. K.; Cruz, W. A.; Moitzi, C.; Lindner, P.; Arêas, E. P. G.; Schurtenberger, P., *J. Phys. Chem. B* **2010,** *114*, 11875-11883.
28. Loo, R. R. O.; Lakshmanan, R.; Loo, J. A., *J. Am. Soc. Mass Spectrom.* **2014,** *25*, 1675-1693.
29. Chrisman, P. A.; Newton, K. A.; Reid, G. E.; Wells, J. M.; McLuckey, S. A., *Rapid Commun. Mass Spectrom.* **2001,** *15*, 2334-2340.
30. Qin, J.; Perera, R.; Lovelace, L. L.; Dawson, J. H.; Lebioda, L., *Biochemistry* **2006,** *45*, 3170-3177.
31. Li, Q.; Mabrouk, P., *J. Biol. Inorg. Chem.* **2003,** *8*, 83-94.
32. Kuper, J.; Wong, T. S.; Roccatano, D.; Wilmanns, M.; Schwaneberg, U., *J. Am. Chem. Soc.* **2007,** *129*, 5786-5787.
33. Bornschein, R. E.; Niu, S.; Eschweiler, J.; Ruotolo, B. T., *J. Am. Soc. Mass Spectrom.* **2016,** *27*, 41-49.
34. Almira Correia, M.; Sinclair, P. R.; De Matteis, F., *Drug Metab. Rev.* **2011,** *43*, 1-26.
35. Cammarata, M. B.; Brodbelt, J. S., *Chem Sci* **2015,** *6*, 1324-1333.